

Comparative analysis of MPPT techniques for photovoltaic systems: classical, fuzzy logic, and sliding mode approaches

Mohamed El Hafydy, Mohamed Benydir, Elmahni Lahoussine, Elmoutawakil Alaoui My Rachid, Youssef Oubail

Laboratory of Engineering Sciences and Energy Management (LASIME), National School of Applied Sciences, Ibn Zohr University, Agadir, Morocco

Article Info

Article history:

Received Sep 16, 2024

Revised Mar 24, 2025

Accepted Jun 23, 2025

Keywords:

Control

Fuzzy logic

MPPT

Photovoltaic

Sliding mode

ABSTRACT

This study presents a comprehensive comparative analysis of maximum power point tracking (MPPT) strategies for photovoltaic systems, focusing on the classical perturb and observe (P&O) method, an artificial intelligence-based fuzzy logic controller (FLC), and a robust sliding mode control (SMC) technique. These methods aim to maximize power output by dynamically adapting to rapid and unpredictable environmental variations, such as changes in solar irradiance. Simulations performed in the MATLAB/Simulink environment under diverse real-world scenarios demonstrate that SMC and FLC outperform the conventional P&O approach, particularly under conditions of sudden and severe environmental fluctuations. The findings highlight the advanced controllers' ability to sustain optimal power extraction, minimize energy losses, and maintain system stability across varying operating conditions. These results underscore the potential of SMC-based MPPT systems to enhance the efficiency and resilience of renewable energy applications, making them highly viable for deployment in real-world scenarios characterized by volatile environmental conditions.

This is an open access article under the [CC BY-SA](https://creativecommons.org/licenses/by-sa/4.0/) license.



Corresponding Author:

Mohamed El Hafydy

Laboratory of Engineering Sciences and Energy Management (LASIME)

National School of Applied Sciences, Ibn Zohr University

Agadir, Morocco

Email: mohamed.elhafydy@edu.uiz.ac.ma

1. INTRODUCTION

The increasing worldwide need for clean and sustainable energy has intensified the focus on renewable energy sources, particularly solar power. Photovoltaic (PV) systems are at the forefront of this transition, offering a promising solution to meet energy needs while reducing carbon emissions [1]. However, the efficiency of PV systems is inherently limited by their ability to continuously operate at the maximum power point (MPP), which varies due to changing environmental conditions, such as irradiance and temperature. This challenge underscores the importance of effective maximum power point tracking (MPPT) techniques [2]. Significant research has been conducted to enhance the energy efficiency of PVSs by implementing predictive and tracking techniques for maximum power point extraction [3]. A reliable control system consistently tracks the MPP under all environmental conditions, ensuring the system operates at optimal performance. Various MPPT methods have been developed to optimize the energy extraction from PV systems. Among these, the conventional perturb and observe (P&O) [4], incremental conductance (INC) [5], backstepping [6], fuzzy logic (FL) [7], and sliding mode control (SMC) [8]. These methods can be chosen based on performance parameters such as complexity, convergence rate, speed, soft cost, sensor

requirement, and reliability [9]. Typically, MPPT methods adjust a reference signal—positive or negative—based on the operating state of PVSSs. While most techniques perform well in stable conditions, they often struggle when faced with rapid changes in weather or load. Many of these methods are based on the incremental conductance (InCon) and P&O algorithms [10], which rely on PV electrical parameters to determine the MPP. However, these approaches can lead to precision errors due to the time lost during the search for the maximum power point [11]. To address these challenges, an improved MPPT algorithm has been developed, as highlighted in [12]. This enhanced approach combines P&O with FL control, aiming to overcome the limitations of traditional P&O methods. By dynamically adjusting the perturbation amplitude within the P&O algorithm, this technique enhances transient response and minimizes steady-state voltage oscillations, leading to more efficient and reliable power tracking.

Also, Nadkarni *et al.* [13] enhances traditional MPPT methods by modifying the fuzzy logic controller (FLC) and P&O techniques. These improvements aim to reduce steady-state voltage oscillations and improve transient response in photovoltaic systems. Two MPPT methods are compared: P&O and SMC [14]. P&O is generally applied in simple or stand-alone installations, while SMC is better suited for larger systems, so the SMC has gained a lot of attraction in the designing of nonlinear control systems due to its simplicity, robustness, and good dynamic behavior [15]. On the other hand, the SMC technique, chosen for its robustness and low computational complexity, is compared with traditional methods like proportional integral derivative PID and P&O, showing superior performance in handling sudden irradiance changes. Experimental validation on a PV rooftop installation confirmed the approach's effectiveness in maximizing energy output [16]. MPPT algorithms play a crucial role in maximizing power output under varying environmental conditions.

Traditional MPPT techniques, such as the P&O method, often struggle to adapt effectively to rapid and unpredictable changes in solar irradiance [17], leading to suboptimal energy harvesting. To address these limitations, this paper proposes advanced MPPT techniques based on SMC and FLC. SMC is renowned for its robustness against disturbances and uncertainties [18], while FLC offers flexibility in handling nonlinear systems and complex decision-making processes [19]. By leveraging the strengths of both approaches, the proposed controllers aim to enhance the precision, response speed, and overall performance of MPPT in PV systems. This paper aims to evaluate and compare the effectiveness of these three MPPT techniques in maximizing the efficiency of PV systems. By analyzing their performance under varying irradiance levels, the study seeks to identify the most reliable and efficient method for real-world applications in renewable energy systems.

The rest of this article is organized as follows. Section 2 presents the modeling of the PV system and the associated boost converter, establishing the foundational elements necessary for implementing MPPT algorithms. In section 3, the three MPPT techniques P&O, FLC, and SMC are explained in detail, along with their respective design processes. Section 4 offers a simulation study conducted in MATLAB/Simulink, comparing the performance of these three MPPT methods under various conditions.

2. METHOD

2.1. Photovoltaic model

Researchers have developed various models to simulate the behavior of photovoltaic cells under different conditions. Each model builds upon the ideal representation, which consists of a current source to capture solar energy and a diode to reflect the characteristics of the P-N junction. Figure 1 illustrates the equivalent electrical circuit of the one-diode PV model [20]. A photovoltaic cell can be represented as a current source in parallel with a simple P-N diode and a shunt resistor (R_{sh}), all connected in series with a resistance (R_s). Using Kirchhoff's current law, the output current of the solar cell can be given by (1).

$$I_{PV} = I_{ph} - I_d - I_{sh} \quad (1)$$

Based on Shockley's diode equation, I_d is expressed as:

$$I_d = I_0 \left[\exp \left(\frac{V_{pv} + R_s I_{pv}}{n V_T} \right) - 1 \right] \quad (2)$$

$$I_0 = I_{rs} \cdot \left(\frac{T}{T_n} \right)^3 \exp \left[\frac{q E_{g0}}{n K} \times \left(\frac{1}{T_n} - \frac{1}{T} \right) \right] \quad (3)$$

$$I = I_{ph} - I_0 \left[\exp \left(\frac{V_{pv} + R_s I_{pv}}{n V_T} \right) - 1 \right] - \frac{V_{pv} + R_s I_{pv}}{R_{sh}} \quad (4)$$

$$V_T = \frac{kT}{q} \quad (5)$$

where I_{PV} is the output terminal current, I_{ph} is the photocurrent generated by the cell under standard test conditions (STC) with $G=1000 \text{ W/m}^2$ and $T=25^\circ\text{C}$, I_d is the current passing through the diode, and I_{sh} is the shunt resistor current. I_0 is the saturation current, q is the electron charge, K is the Boltzmann constant, n is the ideality factor relative to the module, and T is the diode junction temperature [21]. Table 1 presents the parameters of the PV model used in this study, specifically the polycrystalline type, with a peak power of 240 Wc under standard test conditions (STC).

$$I_{ph} = [I_{sc} + k_i(T - T_n)] \times \frac{G}{1000} \quad (6)$$

$$I_d = I_{rs} \cdot \left(\frac{T}{T_n}\right)^3 \exp \left[\frac{q E_{g0}}{n \cdot K} \times \left(\frac{1}{T_n} - \frac{1}{T} \right) \right] \quad (7)$$

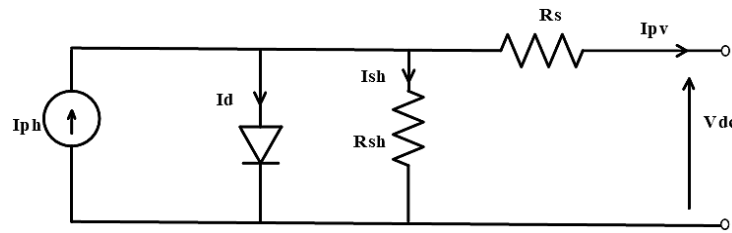


Figure 1. PV cell model

Table 1. PV parametres

Parameters	Values
Maximum power Pmax	240 W
Current at maximum power Ipm	7.9 A
Voltage at maximum power Vpm	30.2 V
Short-circuit current Icc	8.33 A
Open-circuit voltage Voc	37.2 V
Shunt resistance Rsh	1000 Ω
Series resistance Rs	0.008 Ω
Ideality factor n	1.2

2.2. Boost converter

The boost converter is commonly used in renewable energy applications, including solar and wind power. Due to the intermittent nature of solar energy production, it is important to address this variability to enhance overall system efficiency [22]. One significant application of the boost converter is in maximum power point tracking systems. Figure 2 illustrates the structure of a boost converter, which consists of a PV V_{pv} , a controlled switch (T), an inductor (L), a diode (D), a filter capacitor (C), and a load resistance of $R=100 \text{ ohms}$. The converter operates in continuous conduction mode (CCM), with its behavior depending on whether the switch T is conducting or not. As a DC/DC converter, the boost converter increases the input voltage to a higher level at the output. It regulates the voltage at the PV panel terminals based on the chosen control strategy, which is implemented by adjusting the duty cycle of the voltage applied to the switch gate (T).

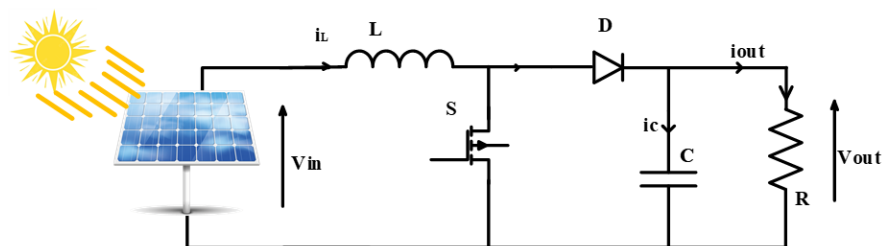


Figure 2. Boost converter

The power flow is regulated by adjusting the duty cycle α of the switching period T_s . Depending on whether the switch (S) is on or off, the converter operates in two distinct states: $S = 0$; $t \in]0; \alpha T_s]$: When the switch is on, the diode is reverse-biased, preventing current flow through it. During this phase, the inductor stores energy by drawing current from the input voltage source, while the capacitor supplies power to the load by discharging through the resistor. The corresponding equations for this state are:

$$V_{pv} - L \frac{di_L}{dt} = 0 \quad (8)$$

$$\frac{V_{out}}{R} - C \frac{dV_{out}}{dt} = 0 \quad (9)$$

the two equations above can be presented in matrix form as (10).

$$\begin{bmatrix} \frac{di_L}{dt} \\ \frac{dV_{out}}{dt} \end{bmatrix} = \begin{bmatrix} 0 & 0 \\ 0 & \frac{-1}{RC} \end{bmatrix} \begin{bmatrix} i_L \\ V_{out} \end{bmatrix} + \begin{bmatrix} \frac{1}{L} \\ 0 \end{bmatrix} V_{pv} \quad (10)$$

$S = 0$; $t \in [\alpha T_s; T_s]$ when the switch is off, the diode D becomes forward-biased, allowing current to flow through it. During this phase, the energy stored in the inductor L is transferred to the capacitor C, which helps maintain the output voltage. The equations for this stage are:

$$V_{pv} - V_{out} - L \frac{di_L}{dt} = 0 \quad (11)$$

$$i_L - \frac{V_c}{R} - C \frac{dV_{out}}{dt} = 0 \quad (12)$$

the two in (11) and (12) can also be presented in matrix form as (13).

$$\begin{bmatrix} \frac{di_L}{dt} \\ \frac{dV_{out}}{dt} \end{bmatrix} = \begin{bmatrix} 0 & \frac{-1}{L} \\ \frac{1}{C} & \frac{-1}{RC} \end{bmatrix} \begin{bmatrix} i_L \\ V_{out} \end{bmatrix} + \begin{bmatrix} \frac{1}{L} \\ 0 \end{bmatrix} V_{pv} \quad (13)$$

The state-space averaging technique helps derive a simplified model of the converter over a full switching period. Essentially, this approach replaces the instantaneous state-space representation with an averaged model that captures the circuit's overall behavior throughout T_s . Applying this method, the modified averaged model is expressed as:

$$A = A_1\alpha + A_2(1 - \alpha) \quad (14)$$

$$B = B_1\alpha + B_2(1 - \alpha) \quad (15)$$

where the matrices A_1 , A_2 , B_1 , and B_2 are given by (16).

$$A_1 = \begin{bmatrix} 0 & 0 \\ 0 & \frac{-1}{RC} \end{bmatrix} A_2 = \begin{bmatrix} 0 & \frac{-1}{L} \\ \frac{1}{C} & \frac{-1}{RC} \end{bmatrix} B_1 = \begin{bmatrix} \frac{1}{L} \\ 0 \end{bmatrix} B_2 = \begin{bmatrix} \frac{1}{L} \\ 0 \end{bmatrix} \quad (16)$$

Using the equations above to obtain the averaged state-space model of the converter over the entire period T_s .

$$\begin{bmatrix} \frac{di_L}{dt} \\ \frac{dV_{out}}{dt} \end{bmatrix} = \begin{bmatrix} 0 & \frac{-(1-\alpha)}{L} \\ \frac{(1-\alpha)}{C} & \frac{-1}{RC} \end{bmatrix} \begin{bmatrix} i_L \\ V_{out} \end{bmatrix} + \begin{bmatrix} \frac{1}{L} \\ 0 \end{bmatrix} V_{pv} \quad (17)$$

Defining the state vector as (18).

$$x = [i_L \quad V_{out}]^T \quad (18)$$

The (17) can be expressed as (19) and (20).

$$\dot{x} = Ax + BV_{in} \quad (19)$$

$$y = Cx \quad (20)$$

Where y is the output vector and the system matrices are defined as in (21).

$$A = \begin{bmatrix} 0 & -\frac{(1-\alpha)}{L} \\ \frac{1-\alpha}{C} & -\frac{1}{RC} \end{bmatrix} \quad B = \begin{bmatrix} \frac{1}{L} \\ 0 \end{bmatrix} \quad C = [01] \quad (21)$$

2.3. MPPT controllers

2.3.1. Perturb and observe method (P&O)

In a photovoltaic system, the P&O method is used to control a DC-DC boost converter, which transforms the fluctuating DC voltage from solar panels into a stable DC output suitable for the load. As illustrated in Figure 3, the P&O algorithm regulates this converter by continuously adjusting the duty cycle α of the switch (S). This ensures that the output voltage remains at the level corresponding to the MPP of the solar panels.

The P&O method is widely used for MPPT in photovoltaic systems due to its simplicity and low dependency on system parameters. It works by periodically adjusting the array voltage (either increasing or decreasing it) and comparing the resulting power with the previous cycle. If the power increases, the perturbation continues in the same direction; otherwise, it reverses. As a result, each MPPT cycle causes a slight fluctuation in the array's terminal voltage. While the P&O algorithm effectively tracks the MPP under stable conditions, it may struggle when atmospheric conditions change gradually or continuously, potentially leading to power loss [23].

2.3.2. Fuzzy logic control (FLC)

Recently, a number of artificial intelligence-inspired strategies have been developed and implemented as MPPT algorithms, often referred to as 'intelligent' due to their robustness and ability to tolerate modeling inaccuracies [24]. Among these strategies is FL. The FL theory allows for the modeling and rigorous processing of imprecise, uncertain, and subjective information, making it particularly suitable for approximating nonlinear functions. However, implementing a fuzzy logic system requires a thorough and complete understanding of the system to accurately establish the inference rules. Designing a fuzzy controller, such as the MAMDANI type used as an MPPT algorithm, involves four key steps: fuzzification, rule definition, fuzzy inference, and defuzzification. These steps are illustrated in Figure 4.

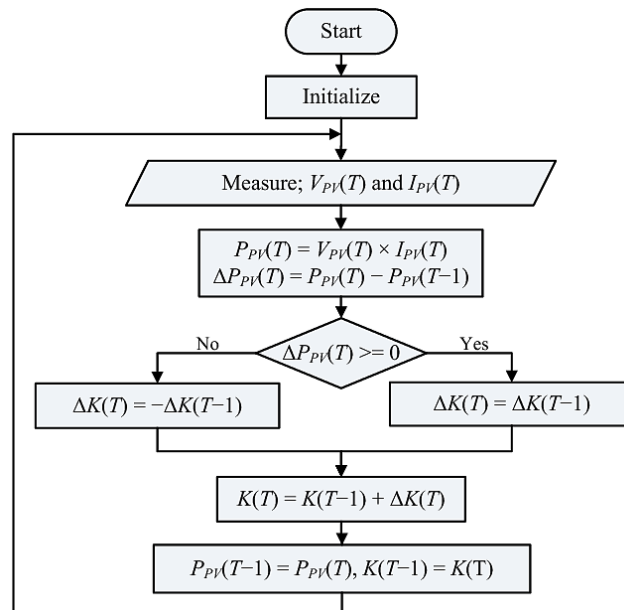


Figure 3. P&O algorithm

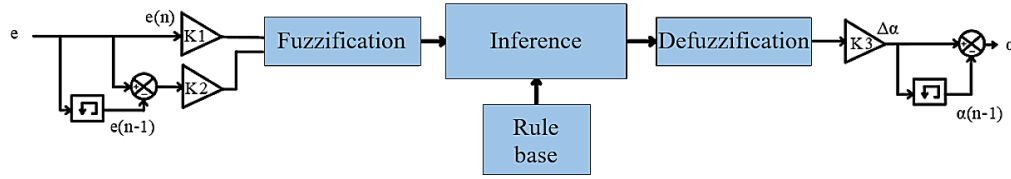


Figure 4. Control structure of MPPT FL

The proposed fuzzy MPPT controller has two inputs and one output. The two input variables of the FLC are the error (e) and the change in error (Δe) measured at each sampling step, while the output variable ($\Delta\alpha$) represents the increment of the duty cycle. The two inputs e and Δe are defined as follows:

$$e = \frac{\Delta V_{pv}}{\Delta I_{pv}} I_{pv} + V_{pv} \quad (22)$$

$$\Delta e = e(n) - e(n-1) \quad (23)$$

where ΔV_{pv} and ΔI_{pv} are respectively the variations in voltage and current of the sources measured at two sampling periods n and $n-1$. The value of the error $e(n)$ actually reflects the system's response in the 'perturb and observe' method, indicating how far it is to the right or left of the optimal value. The value of $\Delta e(n)$ determines the control effort needed to reach the optimum in finite time.

2.3.3. Sliding mode control (SMC)

Sliding mode control (SMC) is a nonlinear control approach initially designed for systems with changing structures. One of its key strengths is its ability to ensure stability while remaining highly robust against significant variations in system parameters or external disturbances. Unlike the classical method used in some works to determine the sliding surface by calculating sliding coefficients, the sliding mode control concept modeled in this study is designed to drive the system to operate at the maximum power point, meaning that the sliding surface is equivalent to the MPP condition [25].

The first step in designing the control involves selecting the sliding surface. This surface can be chosen as (24).

$$\frac{dP_{pv}}{dI_{pv}} = \frac{dI_{pv}^2 R_{pv}}{dI_{pv}} = I_{pv} \left(2R_{pv} + I_{pv} \frac{dR_{pv}}{dI_{pv}} \right) = 0 \quad (24)$$

Knowing that the maximum power point (MPP) condition is given by (25).

$$\frac{dP_{pv}}{dI_{pv}} = 0 \quad (25)$$

Where $R_{pv} = \frac{V_{pv}}{I_{pv}}$ is the equivalent load connected to the PV and I_{pv} is the PV current. The solution of (25) is: $2R_{pv} + I_{pv} \frac{dR_{pv}}{dI_{pv}}$. Consequently, the sliding surface is defined as (26).

$$S = 2R_{pv} + I_{pv} \frac{dR_{pv}}{dI_{pv}} \quad (26)$$

Figure 5 illustrates the P-V characteristics and how the MPP shifts along the sliding surface. When examining the P-V characteristics of the PV panel under specific weather conditions, Figure 6 can be divided into two distinct zones, separated by the maximum power point (MPP), where the slope of the curve is zero ($S=0$). Zone 1 corresponds to a positive slope ($S < 0$), while zone 2 corresponds to a negative slope ($S > 0$). For instance, if the operating point is to the left of the MPP, the control should move toward the sliding surface by increasing the PV voltage V_{pv} . Conversely, if the operating point is to the right of the MPP, the control should adjust toward the sliding surface by decreasing V_{pv} . To achieve this, the switching control law is defined by (27).

$$\alpha = \begin{cases} \alpha + \Delta\alpha & \text{if } S > 0 \\ \alpha - \Delta\alpha & \text{if } S < 0 \end{cases} \quad (27)$$

Consider a time-dependent nonlinear switching system defined by (28).

$$\dot{x}(t) = g(x(t)) + \varphi(x(t)) \cdot \alpha_{eq} \quad (28)$$

The equivalent control is determined from (29).

$$\dot{S} = \left[\frac{dS}{dx} \right]^T \dot{X} = \left[\frac{dS}{dx} \right]^T (f(X) + g(X)) \alpha_{eq} \quad (29)$$

The equivalent control can be obtained from (30).

$$\alpha_{eq} = \frac{\left[\frac{dS}{dx} \right]^T f(X)}{\left[\frac{dS}{dx} \right]^T g(X)} = 1 - \frac{V_e}{V_s} \quad (30)$$

The Lyapunov function is defined by (31).

$$V = \frac{1}{2} S^2 \quad (31)$$

For the surface $S=0$ to be attractive, it is sufficient for the derivative with respect to V to be negative.

$$\dot{V} = \dot{S}S; \forall S \neq 0 \quad (32)$$

To find this sliding mode existence theorem, we calculate the derivative of the surface S .

$$\dot{S} = \left[\frac{dS}{dx} \right]^T \dot{X} = \left(3 \frac{dR_{pv}}{dI_{pv}} + I_{pv} \frac{\partial^2 R_{pv}}{\partial^2 I_{pv}} \right) \dot{X} \quad (33)$$

The equivalent duty cycle must lie in $0 < \alpha_{eq} < 1$. The real control signal α is proposed as (34).

$$\alpha = 1 \text{ if } \alpha_{eq} + k * S \geq 1$$

$$\alpha = \alpha_{eq} + k * S \text{ if } 0 < \alpha_{eq} + k * S \leq 1$$

$$\alpha = 0 \text{ if } \alpha_{eq} + k * S \leq 0 \quad (34)$$

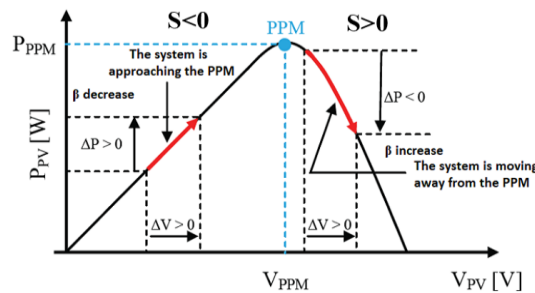


Figure 5. P-V characteristics

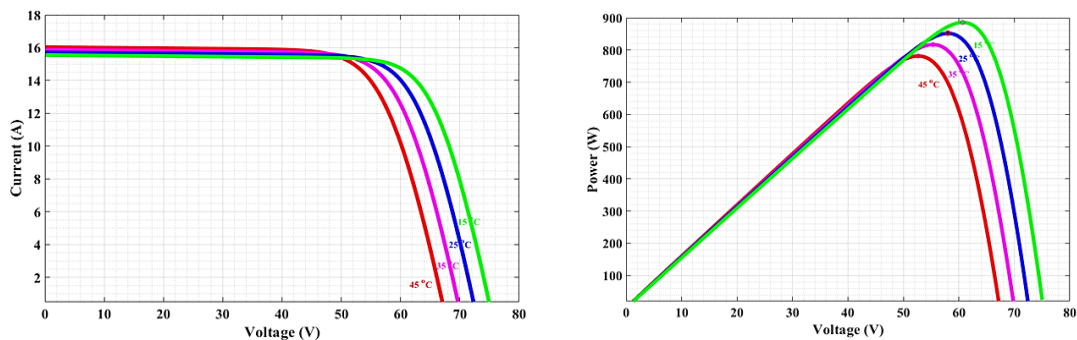


Figure 6. I-V and P-V characteristic curve of the solar cell under fixed irradiance and at different temperatures

3. RESULTS AND DISCUSSION

This section presents the simulation results of the proposed MPPT method based on FLC and SMC. To evaluate the robustness and response speed of the controllers, the simulation involves varying the irradiance of the PV panel over a 1-second period. The simulations were conducted using MATLAB Simulink. We begin by presenting the V-I and P-I characteristics of the PV model used in this study. The characteristic curves of the photovoltaic system show the correlation between current and voltage, and between power and voltage. These nonlinear curves depend on the level of solar irradiance and the temperature of the cell. Figure 7 shows the I-V characteristic curve of the solar cell under fixed irradiance and at different temperatures, and Figure 8 under fixed temperature and at different irradiance. To evaluate the effectiveness of the proposed control techniques for MPPT, Figure 8 shows the irradiance profile subjected to sudden variations. The irradiance rapidly changes between 1000 W/m² and 700 W/m², while the temperature is kept constant at 25 °C.

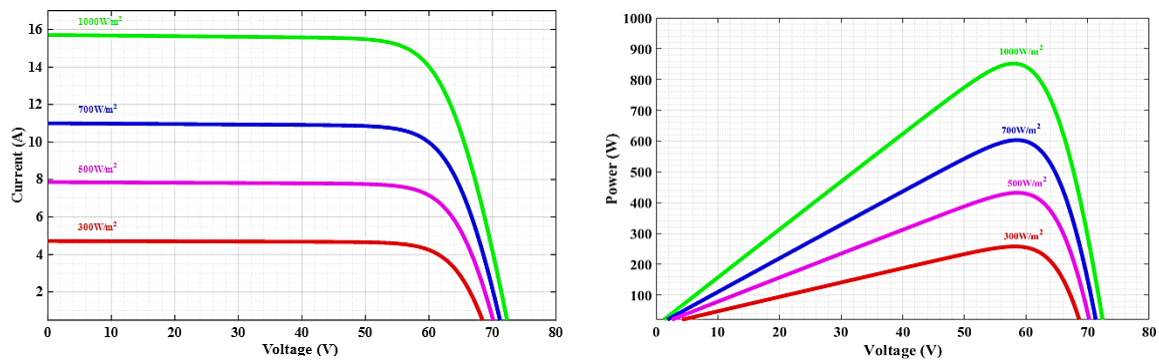


Figure 7. I-V and P-V characteristic curve of the solar cell under fixed temperature and at different irradiance

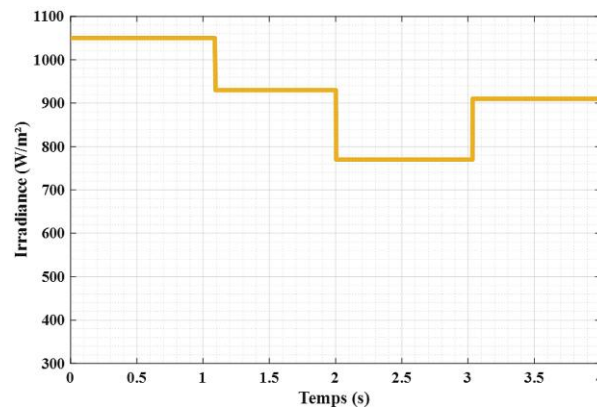


Figure 8. Irradiance profile

Figures 9 through 13 provide a comprehensive evaluation of the MPPT performance across three methods: P&O, FLC, and SMC. Figure 9 illustrates the photovoltaic system's response without any MPPT regulation, revealing a significant discrepancy between the actual power output and the potential power that could be achieved using an MPPT controller. This highlights the substantial energy losses due to the lack of optimal MPP tracking. Figures 10 to 12 showcase the system's performance with the P&O, FLC, and SMC methods, respectively. The P&O method, as depicted in Figure 10, is characterized by oscillations around the MPP. During sudden changes in irradiance, the P&O algorithm requires time to reestablish the MPP, resulting in temporary power losses. These oscillations and delays illustrate the method's limitations in responsiveness and accuracy under dynamic environmental conditions.

In contrast, Figure 11 shows that the FLC method provides effective and stable tracking of the maximum power point, demonstrating its robustness and adaptability to varying conditions. Finally, Figure 12 highlights the SMC-based MPPT method, which achieves precise and efficient tracking of the MPP. This figure underscores the superior performance and reliability of SMC, particularly in fluctuating environmental conditions, offering a significant advantage in maintaining optimal power output.

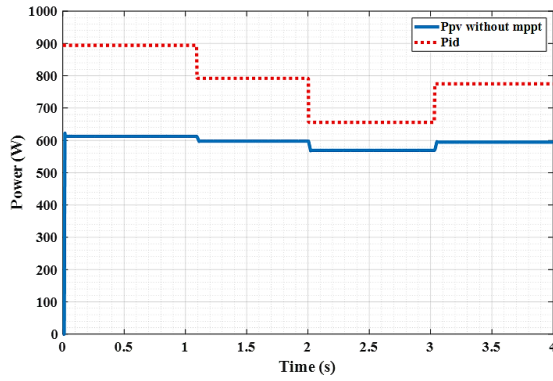


Figure 9. PV response without MPPT

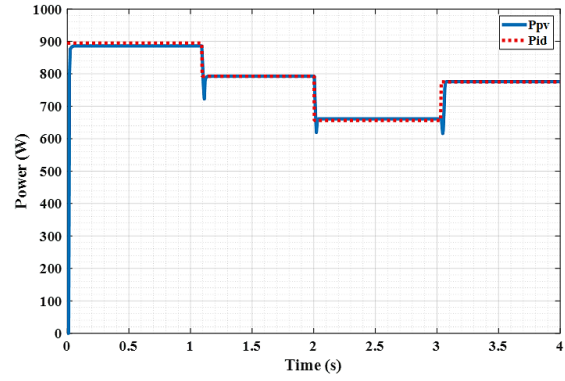


Figure 10. MPPT with P&O

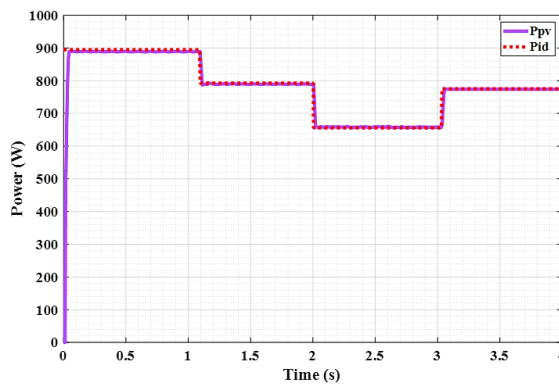


Figure 11. MPPT with FLC

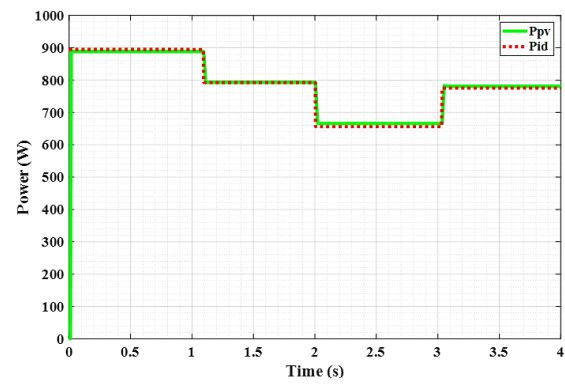


Figure 12. MPPT with SMC

Figure 13 presents a comparison of the three MPPT control methods applied to the photovoltaic system. These methods were evaluated under a change in irradiance from 1000 W/m^2 to 800 W/m^2 . In the transient regime, all three methods exhibit similar response times, with the SMC method showing a slight advantage in speed compared to the P&O and FLC methods. In the steady-state regime, all three methods effectively track the desired power reference. However, a notable difference is observed in the P&O method, which exhibits oscillations around the reference power, while the FLC and SMC methods maintain a smoother tracking performance.

To more precisely evaluate the quality of each method, a statistical analysis was conducted using the mean absolute percentage error (MAPE). This indicator quantifies the magnitude of the error as a percentage, providing an objective and comparative assessment of the performance of the different methods [25]. The calculation of this index is based on the relative error equation in (35).

$$\text{MAPE} = \frac{1}{N} \sum_{t_0}^N \left| \frac{P_{\text{out}} - P_{\text{ref}}}{P_{\text{out}}} \right| * 100 \quad (35)$$

Furthermore, to determine the efficiency of each MPPT controller in terms of power, the efficiency is calculated relative to the maximum power that a PV system could theoretically produce. This efficiency, denoted as η_{MPPT} , is defined as (36).

$$\eta_{\text{MPPT}} = \frac{\int_0^t P_{\text{out}}(t) dt}{\int_0^t P_{\text{max}}(t) dt} \quad (36)$$

The results of the statistical analysis confirmed that the MPPT controller based on sliding mode control is more accurate (MAPE = 2.64%) compared to the controller based on the P&O algorithm (MAPE = 11.25%) and FLC (MAPE = 3.1%). Table 2 presents the efficiency and MAPE of each maximum power point tracking (MPPT) technique for the proposed photovoltaic system: the MPPT based on the P&O method and the MPPT based on FLC and SMC. The results clearly indicate that the SMC-based MPPT achieves

a higher efficiency ($\eta_{\text{MPPT}} = 98.11\%$) compared to the P&O-based MPPT ($\eta_{\text{MPPT}} = 92.83\%$) and FLC ($\eta_{\text{MPPT}} = 95.32\%$). This means that SMC is more effective at extracting the maximum power from the solar system, allowing for better utilization of renewable energy resources and more optimal energy production. The superior performance of SMC in terms of efficiency indicates that it can more accurately track the maximum power point of the photovoltaic system.

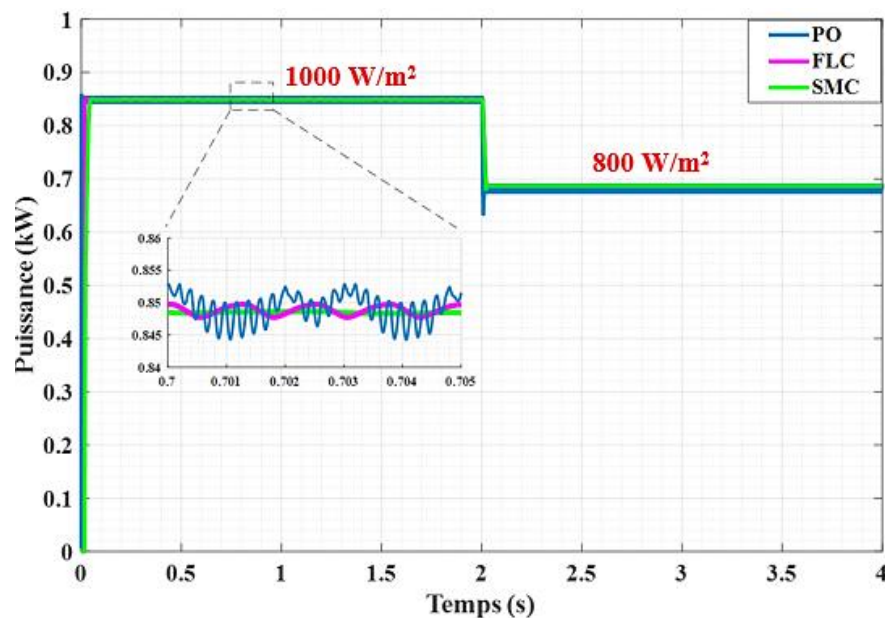


Figure 13. Comparison of the three MPPT control methods

Table 2. MAPE and the efficiency of each MPPT

Control method	MAPE	Efficiency
P&O	11.25%	92.83%
FLC	3.1%	95.32%
SMC	2.64%	98.11%

4. CONCLUSION

This study provides a thorough evaluation of three MPPT techniques: perturb and observe (P&O), fuzzy logic control (FLC), and sliding mode control (SMC) for optimizing photovoltaic system performance. While all three methods demonstrated the ability to effectively track the maximum power point, the SMC-based MPPT method clearly distinguished itself with superior accuracy and efficiency. This enhanced performance suggests that SMC offers a more reliable and robust solution under varying environmental conditions, making it a highly effective approach for improving the efficiency and stability of photovoltaic energy systems. The results of this study highlight the potential of SMC as a leading choice for advancing the performance of renewable energy technologies, particularly in applications where environmental conditions are unpredictable and rapidly changing.

ACKNOWLEDGMENTS

Authors may acknowledge any person, institution, or department that supported to any part of the study.

FUNDING INFORMATION

The authors state no funding involved.

AUTHOR CONTRIBUTIONS STATEMENT

This journal uses the Contributor Roles Taxonomy (CRediT) to recognize individual author contributions, reduce authorship disputes, and facilitate collaboration.

Name of Author	C	M	So	Va	Fo	I	R	D	O	E	Vi	Su	P	Fu
Mohamed El Hafydy	✓	✓				✓	✓	✓	✓				✓	
Mohamed Benydir	✓				✓				✓					✓
Elmahni Lahoussine	✓			✓						✓	✓	✓	✓	
Elmoutawakil Alaoui		✓			✓					✓	✓	✓	✓	
My Rachid														
Youssef Oubail	✓		✓			✓				✓				

C : **C**onceptualization

M : **M**ethodology

So : **S**oftware

Va : **V**alidation

Fo : **F**ormal analysis

I : **I**nvestigation

R : **R**esources

D : **D**ata Curation

O : Writing - **O**riginal Draft

E : Writing - Review & **E**editing

Vi : **V**isualization

Su : **S**upervision

P : **P**roject administration

Fu : **F**unding acquisition

CONFLICT OF INTEREST STATEMENT

The authors state no conflict of interest.

INFORMED CONSENT

We have obtained informed consent from all individuals included in this study.

ETHICAL APPROVAL

The research related to human use has been complied with all the relevant national regulations and institutional policies in accordance with the tenets of the Helsinki Declaration and has been approved by the authors' institutional review board or equivalent committee.

DATA AVAILABILITY

All data supporting the findings of this study were generated through MATLAB/Simulink simulations. The data are available from the corresponding author, [ME], upon reasonable request.




REFERENCES

- [1] M. Dashtdar *et al.*, "Improving the power quality of island microgrid with voltage and frequency control based on a hybrid genetic algorithm and PSO," *IEEE Access*, vol. 10, pp. 105352–105365, 2022, doi: 10.1109/ACCESS.2022.3201819.
- [2] R. B. Bollipo, S. Mikkili, and P. K. Bonthagorla, "Critical review on PV MPPT techniques: classical, intelligent and optimisation," *IET Renewable Power Generation*, vol. 14, no. 9, pp. 1433–1452, Jul. 2020, doi: 10.1049/iet-rpg.2019.1163.
- [3] A. Raj, S. R. Arya, and J. Gupta, "Solar PV array-based DC–DC converter with MPPT for low power applications," *Renewable Energy Focus*, vol. 34, pp. 109–119, Sep. 2020, doi: 10.1016/j.ref.2020.05.003.
- [4] S. Mouslim, M. Oubella, M. Ajaamoum, E. M. Boulaoutaq, M. Benydir, and K. Dahmane, "Comparative analysis of maximum power point tracking method using sliding mode and P&O controllers," *Journal of Theoretical and Applied Information Technology*, vol. 100, no. 14, pp. 5201–5211, 2022.
- [5] A. Lemmassi, A. Derouich, A. Hanafi, A. Byou, M. Benmessaoud, and N. El Ouanjli, "Low-cost MPPT for triple-junction solar cells used in nanosatellites: A comparative study between P&O and INC algorithms," *e-Prime - Advances in Electrical Engineering, Electronics and Energy*, vol. 7, p. 100426, Mar. 2024, doi: 10.1016/j.prime.2024.100426.
- [6] H. Yatimi, Y. Ouberr, S. Chahid, and E. Aroudam, "Control of an off-grid PV system based on the backstepping MPPT controller," *Procedia Manufacturing*, vol. 46, pp. 715–723, 2020, doi: 10.1016/j.promfg.2020.03.101.
- [7] N. Zhani and H. Mahmoudi, "Comparison of the performance of MPPT control techniques (fuzzy logic, incremental conductance and perturb & observe) under MATLAB/Simulink," *IFAC-PapersOnLine*, vol. 58, no. 13, pp. 617–623, 2024, doi: 10.1016/j.ifacol.2024.07.551.
- [8] M. Mohammadinodoushan, R. Abbassi, H. Jerbi, F. Waly Ahmed, H. Abdalqadir Khahmed, and A. Rezvani, "A new MPPT design using variable step size perturb and observe method for PV system under partially shaded conditions by modified shuffled frog leaping algorithm- SMC controller," *Sustainable Energy Technologies and Assessments*, vol. 45, p. 101056, Jun. 2021, doi: 10.1016/j.seta.2021.101056.
- [9] F. F. Ahmad, C. Ghenai, A. K. Hamid, and M. Bettayeb, "Application of sliding mode control for maximum power point tracking of solar photovoltaic systems: a comprehensive review," *Annual Reviews in Control*, vol. 49, pp. 173–196, 2020, doi: 10.1016/j.arcontrol.2020.04.011.




- [10] H. Wang, L. Li, H. Ye, and W. Zhao, "Enhancing MPPT efficiency in PV systems under partial shading: A hybrid POA&PO approach for rapid and accurate energy harvesting," *International Journal of Electrical Power & Energy Systems*, vol. 162, p. 110260, Nov. 2024, doi: 10.1016/j.ijepes.2024.110260.
- [11] S. Senthilkumar *et al.*, "A review on MPPT algorithms for solar PV systems," *International Journal of Research - GRANTHAALAYAH*, vol. 11, no. 3, Apr. 2023, doi: 10.29121/granthaalayah.v11.i3.2023.5086.
- [12] K. Dahmane *et al.*, "Hybrid MPPT control: P&O and neural network for wind energy conversion system," *Journal of Robotics and Control (JRC)*, vol. 4, no. 1, pp. 1–11, Jan. 2023, doi: 10.18196/jrc.v4i1.16770.
- [13] S. S. Nadkarni, S. Angadi, and A. B. Raju, "Simulation and analysis of MPPT algorithms for solar PV based charging station," in *2018 International Conference on Computational Techniques, Electronics and Mechanical Systems (CTEMS)*, Dec. 2018, pp. 45–50, doi: 10.1109/CTEMS.2018.8769191.
- [14] H. Afghoul, D. Chikouche, F. Krim, and A. Beddar, "A comparative study between sliding mode controller and P&O controller applied to MPPT," in *2013 International Renewable and Sustainable Energy Conference (IRSEC)*, Mar. 2013, pp. 112–117, doi: 10.1109/IRSEC.2013.6529701.
- [15] S. P. J. and A. E. Daniel, "Robust sliding mode control strategy applied to IFOC induction motor drive," in *2021 Fourth International Conference on Electrical, Computer and Communication Technologies (ICECCT)*, Sep. 2021, pp. 1–6, doi: 10.1109/ICECCT52121.2021.9616948.
- [16] P. Fernández-Bustamante, I. Calvo, E. Villar, and O. Barambones, "Centralized MPPT based on sliding mode control and XBee 900 MHz for PV systems," *International Journal of Electrical Power & Energy Systems*, vol. 153, p. 109350, Nov. 2023, doi: 10.1016/j.ijepes.2023.109350.
- [17] S. Motahhir, A. El Hammoui, and A. El Ghzizal, "The most used MPPT algorithms: review and the suitable low-cost embedded board for each algorithm," *Journal of Cleaner Production*, vol. 246, p. 118983, Feb. 2020, doi: 10.1016/j.jclepro.2019.118983.
- [18] B. Mbarki, F. Fethi, J. Chroua, and A. Zaafour, "Adaptive neuro-fuzzy inference system algorithm-based robust terminal sliding mode control MPPT for a photovoltaic system," *Transactions of the Institute of Measurement and Control*, vol. 46, no. 2, pp. 316–325, Jan. 2024, doi: 10.1177/01423312231173022.
- [19] B. Mohamed, O. M'hend, M. Sana, A. Mohamed, D. Kaoutar, and I. Belkasem, "Implementation and analysis of a fuzzy logic and sliding mode controller on a boost DC/DC converter," *International Journal of Renewable Energy Research*, vol. 13, no. 1, pp. 294–301, 2023, doi: 10.20508/ijrer.v13i1.13862.g8683.
- [20] S. Mouslim, M. Oubella, M. Kourchi, and M. Ajaamoum, "Simulation and analyses of SEPIC converter using linear PID and fuzzy logic controller," *Materials Today: Proceedings*, vol. 27, pp. 3199–3208, 2020, doi: 10.1016/j.matpr.2020.04.506.
- [21] K. Loukil, H. Abbes, H. Abid, M. Abid, and A. Toumi, "Design and implementation of reconfigurable MPPT fuzzy controller for photovoltaic systems," *Ain Shams Engineering Journal*, vol. 11, no. 2, pp. 319–328, Jun. 2020, doi: 10.1016/j.asej.2019.10.002.
- [22] S. R. Hole and A. D. Goswami, "Quantitative analysis of DC–DC converter models: a statistical perspective based on solar photovoltaic power storage," *Energy Harvesting and Systems*, vol. 9, no. 1, pp. 113–121, Jan. 2022, doi: 10.1515/ehs-2021-0027.
- [23] S. S. Manek, G. S. Mada, and Y. P. K. Kelen, "Pre-eclampsia diagnosis expert system using fuzzy inference system Mamdani," *Jurnal Techno Nusa Mandiri*, vol. 20, no. 2, pp. 80–88, Oct. 2023, doi: 10.33480/techno.v20i2.4622.
- [24] S. Mahjoub, S. Labdai, L. Chrifi-Alaoui, S. Drid, and N. Derbel, "Design and implementation of a fuzzy logic supervisory based on SMC controller for a dual input-single output converter," *International Journal of Electrical Power & Energy Systems*, vol. 150, p. 109053, Aug. 2023, doi: 10.1016/j.ijepes.2023.109053.
- [25] V. S. and R. K. K., "MISO converter based control of solar PV system," *Journal of Electrical Engineering and Automation*, vol. 5, no. 1, pp. 80–92, Mar. 2023, doi: 10.36548/jeea.2023.1.006.

BIOGRAPHIES OF AUTHORS






Mohamed El Hafdy    was born in Zagora, Morocco in 1982. He received Master's degree in process and analysis for air quality treatment in from Faculty of Science, Ibn Zohr University, Agadir, Morocco. He is currently pursuing Ph.D. degree in Laboratory of Engineering Sciences and Energy with the National School of Applied Sciences, Ibn Zohr University, Agadir, Morocco. His research interest is artificial intelligence for microgrid management. He can be contacted at email: mohamed.elhafdy@edu.uiz.ac.ma.






Mohamed Benydir    a specialist in Electrical Engineering and Renewable Energies, obtained his doctoral degree from the National School of Applied Sciences (ENSA) in Agadir. Originally from Agadir, Morocco, his research focuses on renewable energy, engineering science, and energy management. He can be contacted at email: mohamed.benydir@edu.uiz.ac.ma.






Elmahni Lahoussine    holds a Ph.D. in Electrical Engineering and Renewable Energy. Winner of ENSET Rabat in 1993. Member of the Laboratory of Materials and Renewable Energy (RMEL), Professor at the Faculty of Science, Ibn Zohr University, Agadir. His research is focused on smart grid, electric vehicles, demand response, energy efficiency, renewable energy integration, energy storage, and distributed resources. He can be contacted at email: l.elmahni@uiz.ac.ma.



Elmoutawakil Alaoui My Rachid    holds a Ph.D. from the University Ibn Zohr Agadir, Morocco, with a Bachelor in Electronics from ENSET, Rabat, and Master's in Industrial Engineering at the ENSA Agadir. His doctoral thesis focused on the defensive software processors. Permanent member in the Engineering Sciences Laboratory and Energy Management. Responsible of Industrial Systems Optimization Research Team, Agadir, Morocco. He can be contacted at email: r.alaoui@uiz.ac.ma.



Youssef Oubail    was born in Agadir, Morocco, in 1994. He holds a doctorate in Electrical Engineering, Automation, and Renewable Energy. He earned his engineering degree in Industrial Engineering in 2017 from the École Nationale des Sciences Appliquées, Ibn Zohr University, Agadir, Morocco. His research focuses on artificial intelligence and robust controllers for the integration of renewable energies within microgrid topologies. He can be contacted at email: youssef.oubail@edu.uiz.ac.ma.